Supporting Information

In-situ reactive coating of metallic and selenophilic Ag_2Se on Se/C cathode materials for high performance Li-Se batteries

Fugen Sun, Yahui Li‡, Zilong Wu‡, Yu Liu, Hao Tang, Xiaomin Li, Zhihao Yue, Lang Zhou**

Institute of Photovoltaics, Nanchang University, 999 Qianhu Road, Nanchang 330031, China.

* To whom correspondence should be addressed. E-mail: sunfugen@ncu.edu.cn (F. Sun), lzhou@ncu.edu.cn (L. Zhou).
‡ These authors contributed equally to this work.

Content:

Figure S1. (a) N_2 adsorption-desorption isotherm curve and (b) BJH pore size distribution of NMCs.

Figure S2. TEM image of NMCs.

Figure S3. (a) XPS survey spectra and (b) high-resolution N*1s* XPS spectra of NMCs.

Figure S4. STEM elemental mapping images of Ag_2Se@Se/NMC.

Figure S5. Photograph of sealed vials of the 0.01 mol/L Li_2Se_6 in DOL/DME solution, the Li_2Se_6/DOL/DME solution after contact with NMCs and Ag_2Se@NMC after 20 h.

Figure S6. EIS of Ag_2Se@Se/NMC and Se/NMC before the first cycle and after the 50th cycle.

Table S1. Powder electrical conductivity of the NMCs, Se/NMC and Ag_2Se@Se/NMC.

Table S2. Comparison of our results with the previously reported works on the Se-based composites.

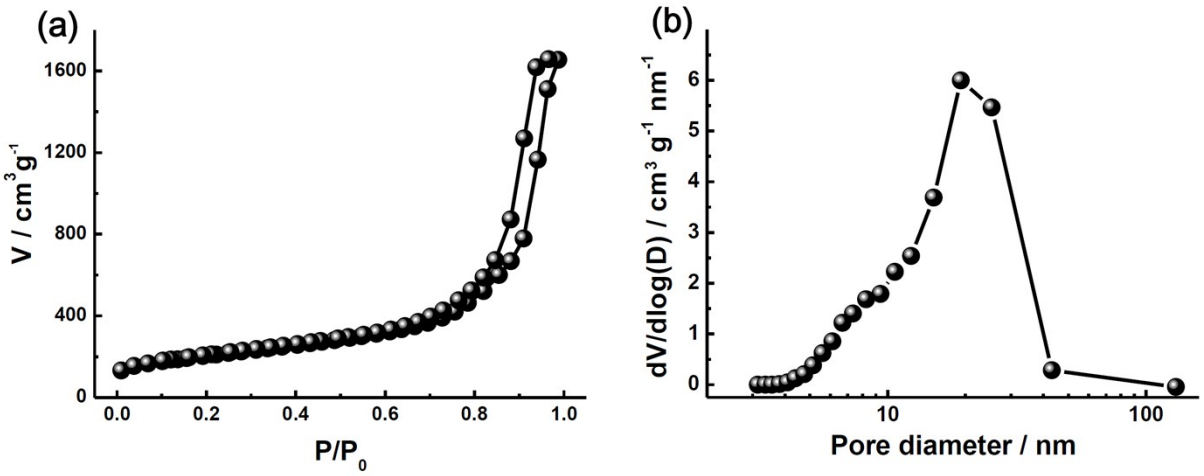

Figure S1. (a) N_2 adsorption-desorption isotherm curve and (b) BJH pore size distribution of NMCs. The isotherm of the NMCs exhibit type IV behaviour following the IUPAC classification, indicating that the NMCs are typically mesoporous carbon materials. The BET surface area and total pore volume are 731 m^2 g^{-1} and 2.6 cm^3 g^{-1}, respectively.

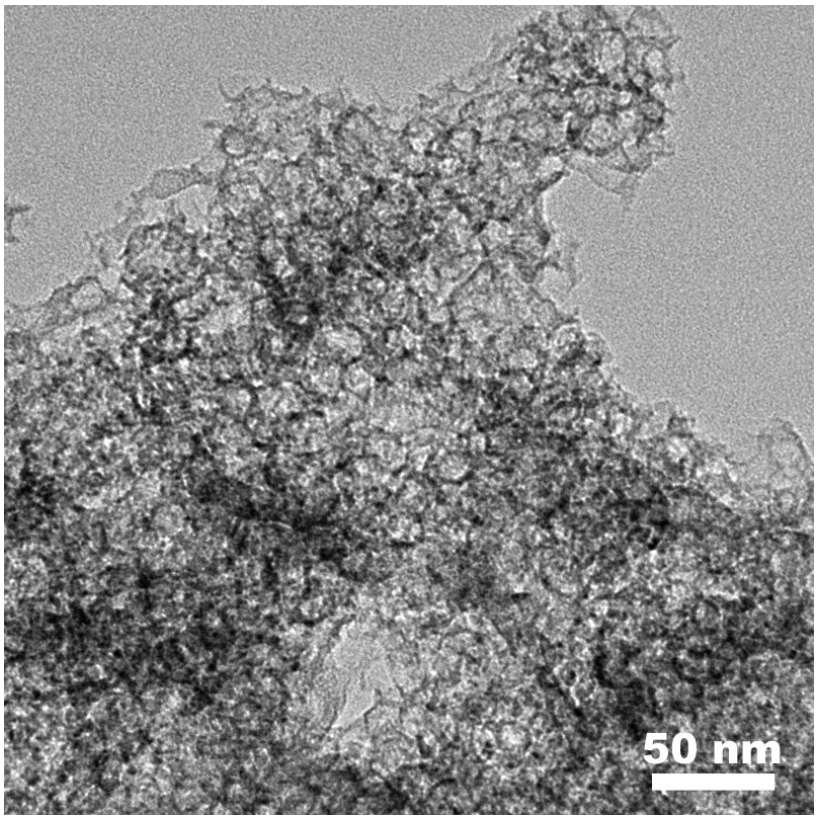

Figure S2. TEM image of NMCs. The NMCs sample consists of developed and spherical mesopores.

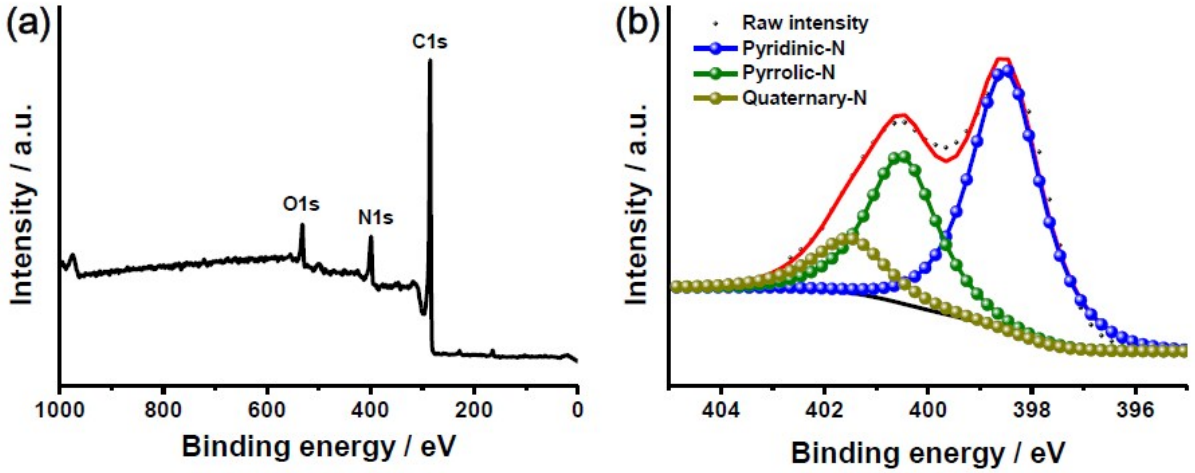

Figure S3. (a) XPS survey spectra and (b) high-resolution N*1s* XPS spectra of NMCs. The XPS survey spectra of the NMCs possess three peaks centered at 284.6, 400.0, and 513.4 eV, corresponding to C*1s*, N*1s*, and O*1s*, respectively, thus excluding the presence of any other impurities. The N*1s* XPS spectra were curve-fitted into three peaks with binding energies of 398.5, 400.5 and 401.6 eV corresponding to pyridinic N, pyrrolic N, and graphitic N, respectively.

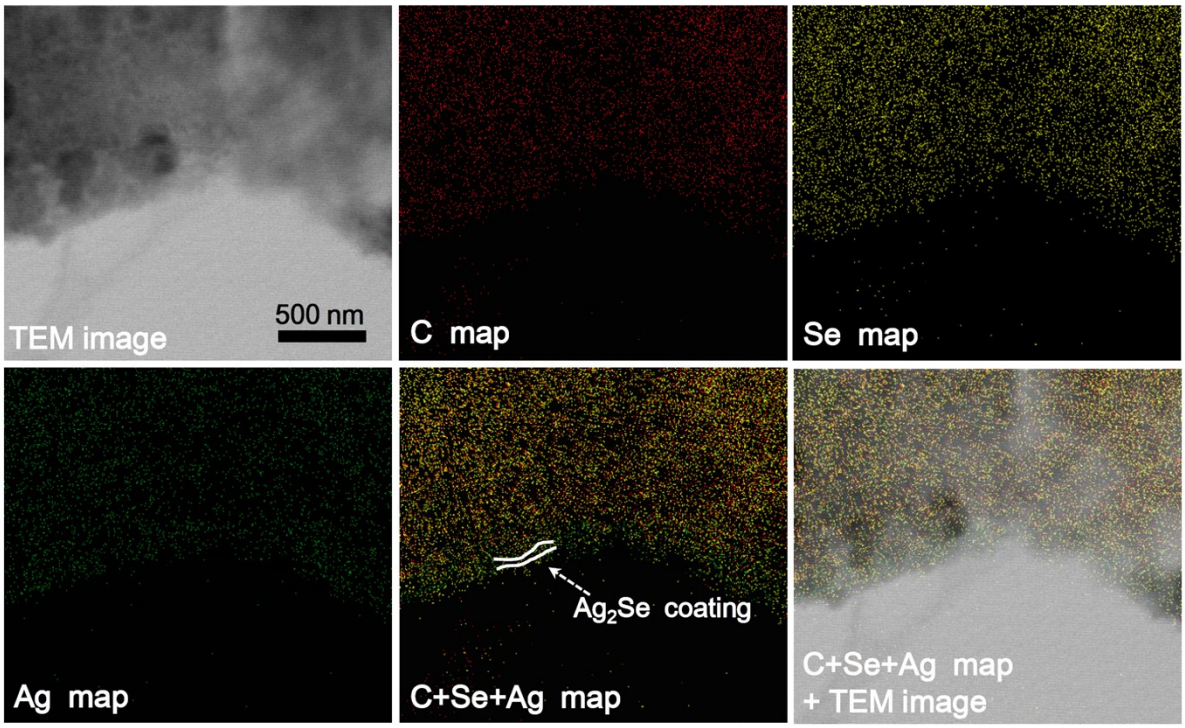

Figure S4. STEM elemental mapping images of Ag_2Se@Se/NMC. From the multi-elemental overlay images of C, Se, Ag, it can be clearly seen that the area of C is a little smaller than those of Se and Ag. The gap between the areas of C and Ag clearly indicates the position of Ag_2Se coating on the surfaces of Se/NMC composites.

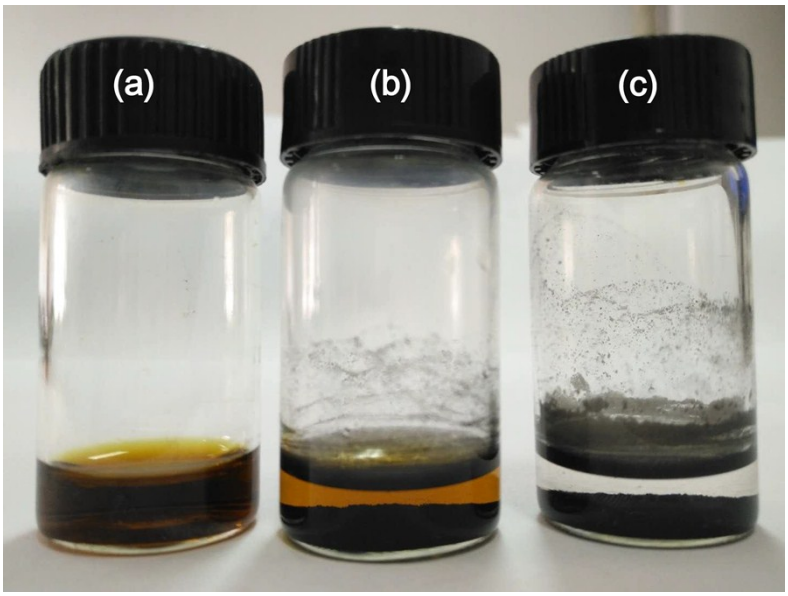

Figure S5. Photograph of sealed vials of the 0.01 mol/L Li_2Se_6 in DOL/DME (1:1, v/v) solution (a), the Li_2Se_6/DOL/DME solution after contact with NMCs (b) and Ag_2Se@NMC (c) after 20 h. The Ag_2Se@NMC samples were obtained by thermal evaporation of Se from Ag_2Se@Se/NMC. It can be clearly observed that the color of the Li_2Se_6 solution changes from dark brown to light brown and transparent color, respectively after absorption by NMCs and Ag_2Se@NMC for 20 h. The significant decoloration of Li_2Se_6 solution after the adsorption of Ag_2Se@NMC confirms the enhanced adsorption capability toward polyselenides of NMCs after Ag_2Se coating.

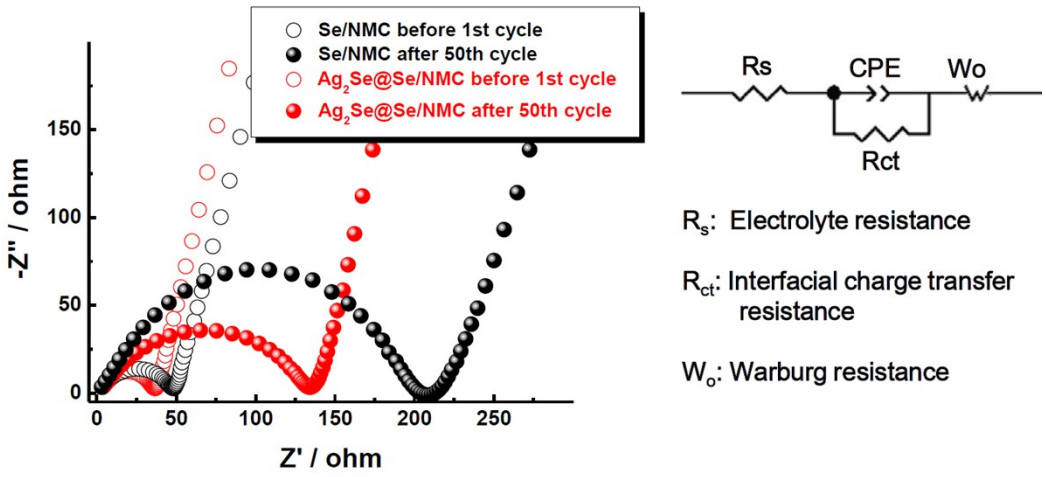

Figure S6. EIS of Ag_2Se@Se/NMC and Se/NMC before the first cycle and after the 50th cycle. R_{ct} is quantified by the x-axis intersect of the semicircle in the high-frequency domain, while W_o is represented by the straight line in the low-frequency region. Upon cycling, the increase of the interfacial charge transfer resistance R_{ct} could be attributed to the decomposition of electrolyte on the electrode surface and the volume variation. More importantly, R_{ct} of Ag_2Se@Se/NMC is lower than that of Se/NMC both before 1st and after 50th cycle, indicating that the interfacial charge transfer of Ag_2Se@Se/NMC is much faster than that of Se/NMC.

Table S1. Powder electrical conductivity of the NMCs, Se/NMC and Ag_2Se@Se/NMC.

Samples	NMCs	Se/NMC	Ag_2Se@Se/NMC
Powder electrical conductivity / S cm^{-1}	0.26	0.21	0.34

Table S2. Comparison of our results with the previously reported works on the Se-based composites.

Composite	Electrolyte	Se loading / wt.%	Current rate	Initial cylce Discharge capacity / mAh g^{-1} (Coulombi cefficiency / %)	Reversible capacity mAh g^{-1}
Se/BPC[1]	DOL/DME	45.1	0.5 C	560 (79.0)	246 (80 cycles)
			1 C	552 (84.4)	264 (80 cycles)
Se/MCN-RGO[2]		62	0.1 C	655 (96.5)	568 (100 cycles)
Se/PPy HS[3]		52.4	0.2 C	630 (94.7)	400 (80 cycles)
Se/CMCs[4]		49.7	0.2 C	780 (80.2)	425 (100 cycles) 308 (460 cycles)
			0.5 C	688 (/)	253 (100 cycles) 239 (200 cycles) 232 (400 cycles) 231 (460 cycles)
Se-NCHPC[5]		56.2	0.5 C	636 (81.3)	330 (30 cycles)
			1 C	535 (90.9)	277 (50 cycles)
Se/PHCS[6]		60	0.1 C	590 (92.6)	338 (50 cycles)
HCPS/Se[7]		41.2	0.5 C	572 (83.9)	299 (100 cycles)
Se-CP[8]		60	1 C	1504 (99)	413 (50 cycles)
meso-C@Se[9]		48	0.5 C	641 (58.0)	301 (100 cycles)
			1 C	661 (/)	320 (100 cycles)
Se@C[10]		68	0.1 C	660 (99)	300 (100 cycles)
Se@RGO[11]		80	0.2 C	533 (98)	352 (100 cycles) 308 (200 cycles)
HPCA/Se[12]		56	0.5 C	587 (46.5)	367 (50 cycles)
Se/C[13]		43.2	0.5 C	558 (69.3)	181 (80 cycles)
MWCNT/Se-S[14]		56.2	0.5 C	646 (79.2)	356 (80 cycles)
3DG-CNT@Se[15]		51	0.2 C	633 (93.4)	531 (100 cycles) 504 (150 cycles)

TiO_2-Se[16]		70.8	0.1 C	481 (53.0)	158 (50 cycles)
MCM-3.8-Se[17]		49.5	0.5 C	513 (92.4)	300 (100 cycles)
C-Co-N/Se[18]		76.5	0.1 C	672 (97.1)	588 (100 cycles) 574 (200 cycles)
Ag_2Se@ Se/NMC (Our work)		67	0.2 C	652 (97.7)	382 (100 cycles)
			0.5 C	594 (96.9)	358 (100 cycles) 298 (200 cycles) 206 (400 cycles)
			1 C	541 (97.1)	301 (100 cycles) 243 (200 cycles) 193 (400 cycles)
Se/CMK-3[19]	EC/DEC	49	0.1 C	920 (57.8)	600 (50 cycles)
Se/Meso-CS[20]		30	0.25 C	480 (34.9)	476 (100 cycles) 462 (200 cycles) 489 (500 cycles)
Se@N-MPC[21]		50	0.5 C	480 (34.9)	476 (100 cycles) 462 (200 cycles) 489 (500 cycles)
Se-MC[22]		51	0.1 C	920 (57.8)	600 (50 cycles)
Se/CNF[23]		52.3	0.07 C	1022 (61.3)	568 (100 cycles) 570 (200 cycles)
Se/PTCDA-C[24]		54	0.15 C	897 (56.9)	317 (100 cycles)
Se/MPCS[25]		60	0.1 C	663 (57)	643 (100 cycles)
Se/PCS[26]		60	0.5 C	560 (64.5)	456 (100 cycles) 433 (200 cycles)
Se/Micro-C[27]		60	1 C	926 (72.9)	540 (100 cycles)
Se/Micro-CS[28]		70.5	1 C	857.8 (56.5)	463 (100 cycles) 348 (200 cycles)

The comparison between our results and the previously reported works demonstrate that the electrochemical performance of the Ag_2Se@Se/NMC is among the best series of Se-based cathode materials when the key performance indicators including the reversible capacity, the initial coulombic efficiency, the Se loading and the used electrolyte are all considered.

References

[1] Y. Qu, Z. Zhang, Y. Lai, Y. Liu, J. Li, A Bimodal Porous Carbon with High Surface Area Supported Selenium Cathode for Advanced Li-Se Batteries, Solid State Ionics 274 (2015) 71-76

[2] K. Han, Z. Liu, J. Shen, Y. Lin, F. Dai, H. Ye, A Free-standing and Ultralong-life Lithium-selenium Battery Cathode Enabled by 3D Mesoporous Carbon/Graphene Hierarchical Architecture, Adv. Funct. Mater. 25 (2015) 455-463

[3] J. Guo, Z. Wen, G. Ma, J. Jin, W. Wang, Y. Liu, A Selenium@Polypyrrole Hollow

Sphere Cathode for Rechargeable Lithium Batteries, RSC Adv. 5 (2015) 20346-20350
[4] T. Liu, M. Jia, Y. Zhang, J. Han, Y. Li, S. Bao, D. Liu, J. Jiang, M. Xu, Confined Selenium within Metal-organic Frameworks Derived Porous Carbon Microcubes as Cathode for Rechargeable Lithiume-selenium Batteries, J. Power Sources 341 (2017) 53-59
[5] Y. Qu, Z. Zhang, S. Jiang, X. Wang, Y. Lai, Y. Liu, J. Li, Confining Selenium in Nitrogen-containing Hierarchical Porous Carbon for High-rate Rechargeable Lithium-selenium Batteries, J. Mater. Chem. A 2 (2014) 12255-12261
[6] Y. Lai, F. Yang, Z. Zhang, S. Jiang, J. Li, Encapsulation of Selenium in Porous Hollow Carbon Spheres for Advanced Lithium-selenium Batteries, RSC Adv. 4 (2014) 39312-39315
[7] J. Li, X. Zhao, Z. Zhang, Y. Lai, Facile Synthesis of Hollow Carbonized Polyaniline Spheres to Encapsulate Selenium for Advanced Rechargeable Lithium-Selenium Batteries, J Alloys Compounds 619 (2015) 794-799
[8] Z. Yi, L. Yuan, D. Sun, Z. Li, C. Wu, W. Yang, Y. Wen, B. Shan Y. Huang, High-performance Lithium-selenium Batteries Promoted by Heteroatom-doped Microporous Carbon, J. Mater. Chem. A 3 (2015) 3059-3065
[9] Y. Lai, Y. Gan, Z. Zhang, W. Chen, J. Li, Metal-organic Frameworks-derived Mesoporous Carbon for High Performance Lithium-selenium Battery, Electrochim. Acta 146 (2014) 134-141
[10] J. Guo, Q. Wang, C. Qi, J. Jin, Y. Zhu, Z. Wen, One-step Microwave Synthesized Core-shell Structured Selenium@Carbon Spheres as Cathode Materials for Rechargeable Lithium Batteries, Chem. Commun. 52 (2016) 5613-5616
[11] X. Peng, L. Wang, X. Zhang, B. Gao, J. Fu, S. Xiao, K. Huo, P. K. Chu, Reduced Graphene Oxide Encapsulated Selenium Nanoparticles for High-power Lithium-selenium Battery Cathode, J. Power Sources 288 (2015) 214-220
[12] S. Jiang, Z. Zhang, Y. Lai, Y. Qu, X. Wang, J. Li, Selenium Encapsulated into 3D Interconnected Hierarchical Porous Carbon Aerogels for Lithium-selenium Batteries with High Rate Performance and Cycling Stability, J. Power Sources 267 (2014) 394-404
[13] Z. Zhang, X. Yang, Z. Guo, Y. Qu, J. Li, Y. Lai, Selenium/Carbon-rich Core-shell Composites as Cathode Materials for Rechargeable Lithium-selenium Batteries, J. Power Sources 279 (2015) 88-93
[14] X. Wang, Z. Zhang, Y. Qu, G. Wang, Y. Lai, J. Li, Solution-based Synthesis of Multi-walled Carbon Nanotube/selenium Composites for High Performance Lithium-selenium Battery, J. Power Sources 287 (2015) 247-252
[15] J. He, Y. Chen, W. Lv, K. Wen, P. Li, Z. Wang, W. Zhang, W. Qin, W. He, Three-dimensional Hierarchical Graphene-CNT@Se: A Highly Efficient Freestanding Cathode for Li-Se Batteries, ACS Energy Lett. 1 (2016) 16-20
[16] Z. Zhang, X. Yang, X. Wang, Q. Li, Z. Zhang, TiO_2-Se Composites as Cathode Material for Rechargeable Lithium-selenium Batteries, Solid State Ionics 260 (2014) 101-106
[17] L. Liu, Y. Wei, C. Zhang, C. Zhang, X. Li, J. Wang, L. Ling, W. Qiao, D. Long, Enhanced Electrochemical Performances of Mesoporous Carbon Microsphere/selenium Composites by Controlling the Pore-structure and Nitrogen-doping, Electrochim. Acta 153 (2015) 140-148
[18] J. He, W. Lv, Y. Chen, J. Xiong, K. Wen, C. Xu, W. Zhang, Y. Li, W. Qin, W. He, Three-dimensional Hierarchical C-Co-N/Se Derived from Metal-organic Framework as Superior Cathode for Li-Se Batteries, J. Power Sources 363 (2017) 103-109
[19] C. Yang, S. Xin, Y. Yin, H. Ye, J. Zhang, Y. Guo, An Advanced Selenium-carbon Cathode for Rechargeable Lithium-selenium Batteries, Angew. Chem. Int. Ed. 52 (2013)

8363-8368
[20] C. Luo, Y. Xu, Y. Zhu, Y. Liu, S. Zheng, Y. Liu, A. Langrock, C. Wang, Selenium@Mesoporous Carbon Composite with Superior Lithium and Sodium Storage Capacity, ACS Nano 7 (2013) 8003-8010
[21] Y. Jiang, X. Ma, J. Feng, S. Xiong, Selenium in Nitrogen-doped Microporous Carbon Spheres for High-performance Lithium-Selenium Batteries, J. Mater. Chem. A 3 (2015) 4539-4546
[22] Y. Liu, L. Si, X. Zhou, X. Liu, Y. Xu, J. Bao, Z. Dai, A Selenium-confined Microporous Carbon Cathode for Ultrastable Lithium-Selenium Batteries, J. Mater. Chem. A 2 (2014) 17735-17739
[23] L. Zeng, W. Zeng, Y. Jiang, X. Wei, W. Li, C. Yang, Y. Zhu, Y. Yu, A Flexible Porous Carbon Nanofibers-selenium Cathode with Superior Electrochemical Performance for Both Li-Se and Na-Se Batteries, Adv. Energy Mater. 5 (2015) 1401377-1401386
[24] C.Luo, J. Wang, L. Suo, J. Mao, X. Fan, C. Wang, In Situ Formed Carbon Bonded and Encapsulated Selenium Composites for Li-Se and Na-Se Batteries, J. Mater. Chem. A 3 (2015) 555-561
[25] H. Ye, Y. Yin, S. Zhang, Y. Guo, Advanced Se-C Nanocomposites: A Bifunctional Electrode Material for Both Li-Se and Li-ion Batteries, J. Mater. Chem. A 2 (2014) 13293-13298
[26] Z. Li, L. Yin, MOF-derived, N-doped, Hierarchically Porous Carbon Sponges as Immobilizers to Confine Selenium as Cathodes for Li-Se Batteries with Superior Storage Capacity and Perfect Cycling Stability, Nanoscale 7 (2015) 9597-9606
[27] Z. Yi, L. Yuan, D. Sun, Z. Li, C. Wu, W. Yang, Y. Wen, B. Shan, Y. Huang, High-performance Lithium-selenium Batteries Promoted by Heteroatom-doped Microporous Carbon, J. Mater. Chem. A 3 (2015) 3059-3065
[28] Z. Li, L. Yuan, Z. Yi, Y. Liu, Y. Huang, Confined Selenium within Porous Carbon Nanospheres as Cathode for Advanced Li-Se Batteries, Nano Energy **9** (2014) 229-236